

## Interlayer interactions in epitaxial oxide growth: FeO on Pt(111)

Y. J. Kim

*Department of Chemistry, University of Hawaii, Honolulu, Hawaii 96822  
and Materials Sciences Division, Lawrence Berkeley National Laboratory, Berkeley, California 94720*

C. Westphal

*Materials Sciences Division, Lawrence Berkeley National Laboratory, Berkeley, California 94720*

R. X. Ynzunza

*Materials Sciences Division, Lawrence Berkeley National Laboratory, Berkeley, California 94720  
and Department of Physics, University of California-Davis, Davis, California 95616*

H. C. Galloway

*Materials Sciences Division, Lawrence Berkeley National Laboratory, Berkeley, California 94720  
and Department of Physics, University of California-Berkeley, Berkeley, California 94720*

M. Salmeron and M. A. Van Hove

*Materials Sciences Division, Lawrence Berkeley National Laboratory, Berkeley, California 94720*

C. S. Fadley

*Materials Sciences, Division, Lawrence Berkeley National Laboratory, Berkeley, California 94720  
and Department of Physics, University of California-Davis, Davis, California 95616*

(Received 12 March 1997)

We have studied the first monolayer of epitaxial iron oxide on Pt(111) with x-ray photoelectron diffraction and other methods. We confirm a previously proposed superlattice model for this monolayer, but also conclude that the oxide grows as a bilayer of FeO(111) with the oxygen layer outermost, the Fe-O interlayer distance is highly compressed relative to bulk FeO by about 50%, and only one of two possible domains forms due to interlayer interactions between oxygen and platinum. [S0163-1829(97)52520-3]

The epitaxial growth of metal oxides is of high current interest due to its relevance to catalysis, magnetic data storage, high-temperature superconductivity, and the recently discovered “colossal” magnetoresistive materials. We have in this paper studied a particularly simple and prototypical system: the growth of iron oxide on a metal substrate, namely Pt(111). This system has been studied by various techniques previously, including low-energy electron diffraction (LEED),<sup>1-3</sup> scanning tunneling microscopy (STM),<sup>4,5</sup> and most recently near-edge x-ray absorption fine structure (NEXAFS).<sup>6</sup> Overall, it has been concluded that the first monolayer of oxide forms as an Fe-O bilayer with an overall geometry like that of the (111) planes in bulk FeO, and that this bilayer also forms a lateral superlattice or Moiré structure that can be clearly seen in both LEED and STM.<sup>4,5</sup> Figures 1(a) and 1(b) show LEED and STM data obtained in this study that exhibit fine structure and a large-scale periodicity ( $\sim 26$  Å in size), respectively, which are linked to this Moiré pattern. Figure 2 shows the atomic model for this superlattice as proposed by Galloway *et al.*<sup>4,5</sup> and derived from LEED and STM data. Thicker layers of oxide quickly convert to Fe<sub>3</sub>O<sub>4</sub>, and the atomic structure of these has been determined by both LEED (Ref. 3) and x-ray photoelectron diffraction (XPD).<sup>7</sup>

We will concentrate here on the first monolayer of oxide, for which several fundamental questions remain to be an-

swered concerning the structure. Among these are which atom is outermost in the Fe-O bilayer, Fe or O? What is the interplanar spacing between the Fe and O? And finally, is there any evidence in the growth mode(s) of an interaction between the outermost layer of the bilayer (whether it be Fe or O) and the underlying Pt?

To this problem we have applied an experimental system that combines for the first time x-ray photoelectron spectroscopy (XPS), XPD, LEED, and STM in the same ultrahigh vacuum environment.<sup>7</sup> The Pt(111) crystal (oriented to within 0.2°) was cleaned using standard cycles of ion bombardment and annealing in both oxygen and ultrahigh vacuum.<sup>3-5,7</sup> The iron oxide was grown in two steps: 0.9–1.0 monolayers of Fe (as judged by both a quartz crystal thickness monitor and XPS relative intensities) were first deposited on the Pt substrate at ambient temperature. This overlayer was then heated to 980 K in  $4 \times 10^{-6}$  torr of oxygen for about 1 min to form the oxide, using a previously discussed recipe.<sup>1-5</sup> This led to LEED patterns with both the primary sixfold spots of the FeO(111) surface and a rosette of additional fine-structure spots around each one of these, as shown in Fig. 1(a). STM images for this surface also showed both the atomic scale periodicity of the outermost layer of the bilayer, but also the much larger periodicity associated with the Moiré superlattice, as shown in Fig. 1(b). A quantitative analysis of the Fe 2*p* and O 1*s* intensities indicated that the

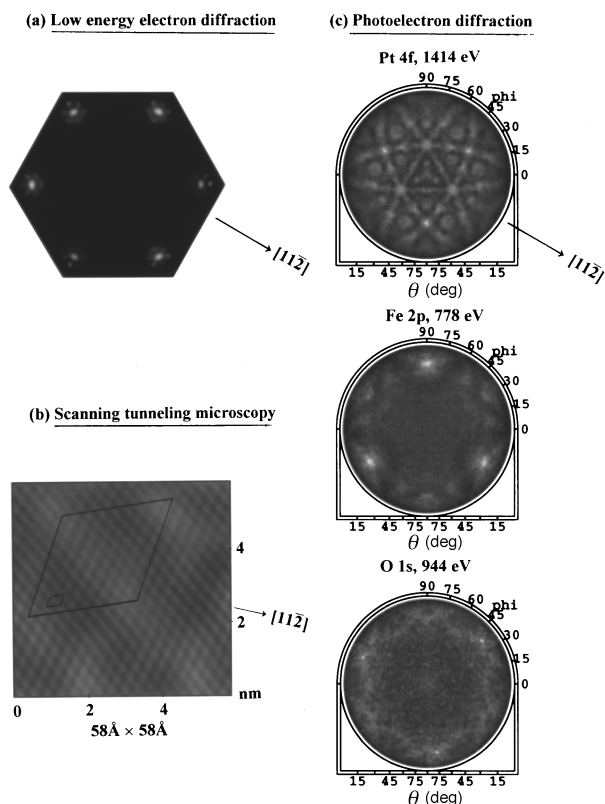


FIG. 1. (a) LEED, (b) STM, and (c) XPD data for 1 ML of FeO on Pt(111). In (c), the full-solid-angle XPD patterns for Pt 4*f*, Fe 2*p*<sub>3/2</sub>, and O 1*s* emission are also shown in stereographic projection.

stoichiometry of the oxide is very close to that of FeO at Fe<sub>1.0</sub>O<sub>1.08</sub>. Nearly full-hemisphere XPD intensity patterns were then measured for all three of the atomic species present using nonmonochromatized Al *K*α radiation for excitation. The photoelectron peaks involved were Pt 4*f* at 1414 eV kinetic energy, Fe 2*p*<sub>3/2</sub> at 777 eV, and O 1*s* at 956 eV, and all three intensities were recorded at each setting of emission direction, thus providing a highly accurate directional relationship among the three patterns. Some typical XPD patterns obtained in this way are shown in Fig. 1(c). The raw data have been normalized by subtracting a smooth instrument function and then dividing by the same function to yield what is often referred to as a  $\chi$  function.<sup>8</sup>

Considering now the XPD data, we can make several observations: The Pt pattern is characteristic of the bulk fcc Pt crystal structure, and it shows both strong forward peaks and Kikuchi-band-like structures that are characteristic of XPD at such high kinetic energies.<sup>8</sup> The Pt pattern permits locating a low-index azimuth such as  $[11\bar{2}]$  in the other two patterns, but it contains no easily derivable information concerning the structure of the oxide bilayer. The Fe pattern by contrast is much simpler, with only three strong peaks separated by 120° in azimuth and at takeoff angles of 20° with respect to the surface, together with weaker fine structure. The anisotropy  $[I_{\max} - I_{\min}]/I_{\max}$  associated with the three strong peaks is large at around 50%. The dominance of forward scattering immediately suggests that each Fe atom has three neighbors above it, with a bond direction of 20° with respect to the surface. This provides a first indication that these neighbors

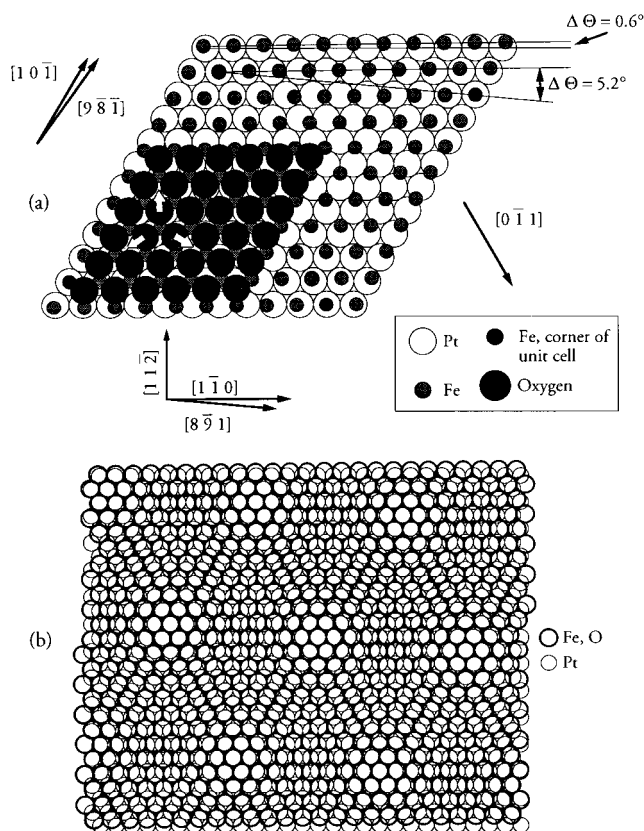


FIG. 2. (a) Structural model for the bilayer of FeO(111) on Pt(111) proposed in Ref. 4. Only a portion of the oxygen atoms in the top layer are shown for clarity. The oxygen termination of the surface was suggested in this prior study, but could not be experimentally verified. The 0.6° rotational mismatch between the overlayer and the Pt substrate in turn leads to a 5.2° mismatch between the lateral superlattice and the substrate; this rotation can occur in both a clockwise and a counterclockwise sense. The white arrows indicate forward scattering directions if iron atoms lie under oxygen as shown. (b) Expanded view of the lateral superlattice formed by the structure in (a), with only the Fe and Pt atoms being shown.

are in the oxygen layer of the bilayer, which would then be outermost. Finally inspecting the O diffraction pattern shows it to have no strong peaks, but only to exhibit a weak sixfold pattern at lower takeoff angles around 16°–24°; the anisotropy in this pattern is also much weaker at only about 12%. This absence of any strong forward scattering peaks for oxygen thus confirms the assignment of the Fe to the bottom of the bilayer and the O to the top. The forward-scattering events responsible for the peaks in the Fe XPD data are indicated by the white arrows superposed on the oxygen atoms in Fig. 2(a). The bilayer is thus indeed like the (111) planes of bulk FeO.

More quantitative structural conclusions can now be drawn by using the measured forward scattering angle of 20° and the lateral spacing between coplanar atoms in the FeO bilayer as derived from either STM or LEED (3.1 Å), together with trivial trigonometry to determine the Fe-O interlayer spacing. The value found is 0.65 Å, which is substantially smaller than the 1.25 Å spacing between Fe and O (111) planes in bulk FeO, although the actual Fe-O bond lengths involved are not so different: 1.95 Å for the bilayer

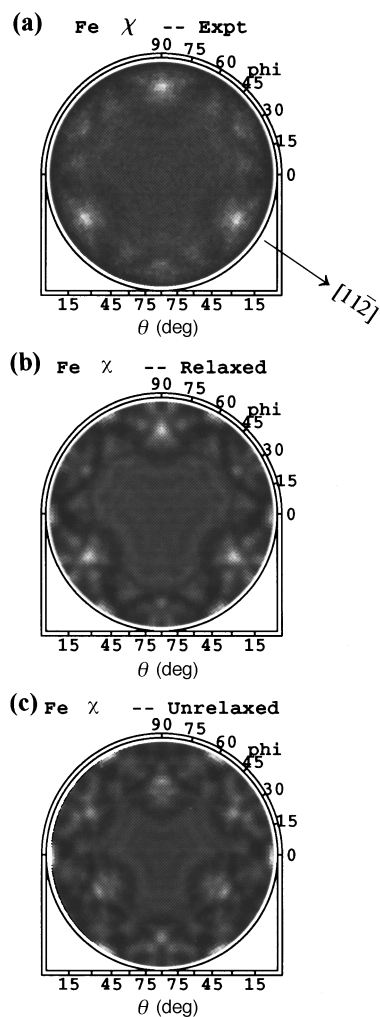


FIG. 3. Experimental and theoretical XPD patterns for Fe  $2p_{3/2}$  emission from 1.0 ML FeO/Pt(111) in stereographic projection: (a) experimental data, (b) theoretical calculation using the cluster of Fig. 2 with an Fe-O bilayer spacing of 0.68 Å, (c) as (b), but with an Fe-O bilayer spacing of 1.25 Å such as that in bulk FeO.

versus 2.15 Å in bulk FeO. Thus, we conclude that there is very different interplanar interaction in this bilayer as compared to that in the bulk material. One possibility is that the interlayer contraction is acting to relieve the large surface dipole that would be present due to the relative negative and positive charges on O and Fe, respectively. We also note that a recent study of this FeO bilayer by Schedel-Niedrig, Weiss, and Schlögl<sup>6</sup> using polarization-dependent NEXAFS has concluded that the interlayer spacing is essentially the same as in bulk FeO. We have thus made a more quantitative analysis of our XPD data, by making an *R*-factor comparison of experiment to the results of single-scattering cluster (SSC) diffraction calculations for a range of interlayer spacings.<sup>8</sup> Single scattering should be an excellent approximation in this bilayer due to the lack of chains of atoms to enhance multiple scattering for all but emission right along the surface. Some of these results for the Fe diffraction pattern are shown in Fig. 3, where experiment is compared to theory for two different Fe-O interplanar spacings: the best-fit contracted 0.68 Å (very close to the 0.65 Å estimate from for-

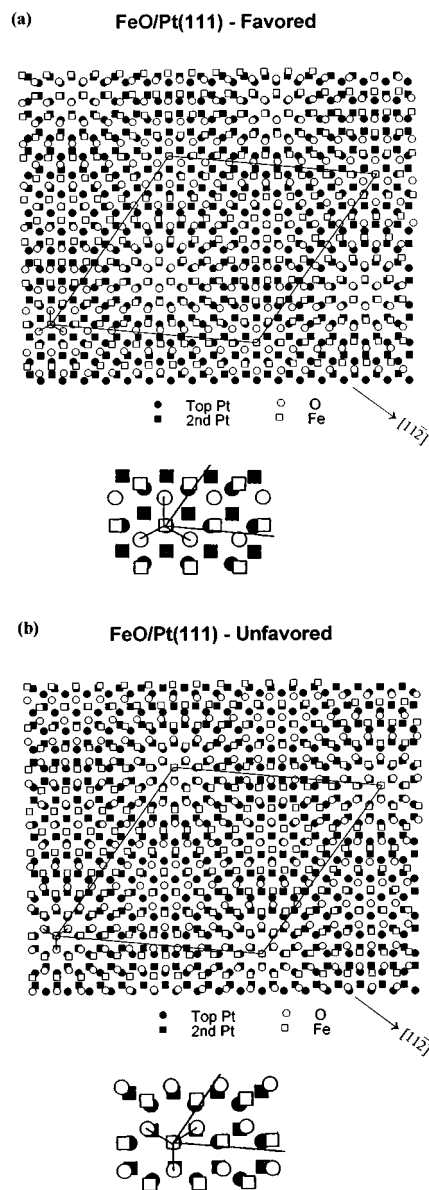


FIG. 4. Two different FeO(111) bilayer structural models linked to the two different possibilities for stacking O with respect to Fe and Pt(111). As viewed from a typical Fe atom, the nearest-neighbor O trimers sit along Pt  $\langle 11\bar{2} \rangle$  directions in (a), and are rotated by 180° in (b). Near the corners of the large unit cells shown, the Fe atoms are directly above first-layer Pt atoms, but in (a) the O atoms do not sit above first- or second-layer Pt atoms, whereas in (b), they sit above second-layer Pt atoms. Also note that some O atoms in the large unit cell sit on top of topmost Pt atoms in (a), while there is no such coincidence in (b).

ward scattering) and the uncontracted 1.25 Å of bulk FeO. The agreement between experiment and theory for 0.68 Å is excellent, including even the weaker features away from the three forward-scattering peaks. For 1.25 Å, the forward-scattering peaks are shifted much too far off the surface, and an additional triplet of strong features that is not present in experiment is also induced. Further consideration of the *R*-factors yields  $0.68 \pm 0.05$  Å for the final result, and confirms the strong contraction of the Fe-O interplanar distance in this bilayer. It has also been pointed out previously<sup>8</sup> that

the use of forward-scattering peaks in this way is expected to be at least twice as accurate for determining bond directions as polarization-dependent NEXAFS, and this may explain the discrepancy with a recent study of this system using the latter method.<sup>6</sup> Additional data supporting this strong contraction comes from theoretical modeling of the STM images by Galloway, Sautet, and Salmeron,<sup>9</sup> in which it is not possible to get agreement between experiment and theory unless a distance very close to 0.68 Å is used. (A separate comparison of experiment and theory for O 1s XPD patterns analogous to that in Fig. 3 also shows excellent agreement, even for the weak hexagonal pattern seen in this data in Fig. 1;<sup>7</sup> however, this pattern is dominated by weaker first-order diffraction effects in *intralayer* scattering from other O atoms, and so is not particularly sensitive to the Fe-O interlayer spacing.)

We can also make a final important conclusion concerning the growth of this oxide bilayer simply by noting that the Fe XPD pattern is clearly *threefold*, rather than sixfold, thus indicating via Fig. 2 that the O layer is always in the same stacking orientation with respect to both the Fe and the underlying Pt. That is, if the Fe-O interaction was all that mattered in the growth of this bilayer, then the entire O layer could be rotated by 60°, or equivalently, flipped in mirror image of itself, so as to yield a second type of growth with the same total bond energy. The two types of domains possible are shown in Fig. 4. Thus, in the limit of no O-Pt interaction, two domains of oxide should grow, with resulting Fe-O bond directions rotated by 60° with respect to one another, and a forward scattering pattern that would be *sixfold*. That the latter clearly does not occur thus leads to the conclusion that one of these two domains or O stacking choices is very strongly favored due to some sort of interlayer O-Fe-Pt interaction. This domain is shown in Fig. 4(a). Although there are many different Fe and O bonding sites relative to Pt, the ensemble of them is clearly different for the two domain types. Further inspection of these two do-

main types indicates that it is necessary to include interactions with *second-layer Pt atoms* to yield an inequivalence between them; thus, at least four layers of atoms must be involved. We suggest that it is a difference in total energy between these domains that is the most likely the cause of the dominance of one, rather than a difference in the kinetics of the growth. It would thus be of interest in the future to carry out theoretical total-energy calculations over the large unit cell of this Moiré pattern in order to better understand the origins of these (and other) interlayer effects on epitaxial oxide growth.

We have thus used x-ray photoelectron diffraction, together with low energy electron diffraction and scanning tunneling microscopy, to study the growth of the first monolayer of iron oxide on Pt(111). This monolayer is confirmed to be a bilayer of Fe and O atoms that forms a large-periodicity Moiré superlattice. Within this bilayer, we have further determined that the oxygen layer is outermost, that the Fe-O interplanar spacing is strongly contracted from that of the analogous planes in bulk FeO, and that interlayer interactions including second-layer Pt atoms also cause one of two possible oxide domain types to be strongly favored. Thus, these results point out several significant structural changes that can occur when metal oxides are grown on a metal substrate, and provide a challenge to theory to quantitatively explain these interactions over such a large unit cell. Our results also illustrate the capability of x-ray photoelectron diffraction to contribute significantly to elucidating such structural changes, especially when used in concert with complementary probes such as LEED and STM.

This work has been supported by the U.S. Department of Energy under Contract No. DOE-AC03-76SF00098 and the U.S. Office of Naval Research under Contract No. N00014-94-0162. We are also very grateful to A.P. Kaduwela for many helpful comments concerning the theoretical analysis of these data.

<sup>1</sup>G. H. Vurens, M. Salmeron, and G. A. Somorjai, *Surf. Sci.* **201**, 129 (1988).

<sup>2</sup>G. H. Vurens, V. Maurice, M. Salmeron, and G. A. Somorjai, *Surf. Sci.* **268**, 170 (1992).

<sup>3</sup>W. Weiss, A. Barbieri, M. A. Van Hove, and G. A. Somorjai, *Phys. Rev. Lett.* **71**, 1884 (1993); A. Barbieri, M. A. Van Hove, and G. A. Somorjai, *Surf. Sci.* **302**, 259 (1994).

<sup>4</sup>H. C. Galloway, J. J. Benitez, and M. Salmeron, *Surf. Sci.* **198**, 127 (1993).

<sup>5</sup>H. C. Galloway, J. J. Benitez, and M. Salmeron, *J. Vac. Sci.*

*Technol. A* **12**, 2302 (1994).

<sup>6</sup>T. Schedel-Niedrig, W. Weiss, and R. Schlögl, *Phys. Rev. B* **52**, 17 449 (1995).

<sup>7</sup>Y. J. Kim, Ph.D. dissertation, University of Hawaii, 1995.

<sup>8</sup>C. S. Fadley, in *Synchrotron Radiation Research: Advances in Surface Science*, edited by R. Z. Bachrach (Plenum, New York, 1992).

<sup>9</sup>H. C. Galloway, P. Sautet, and M. Salmeron, *Phys. Rev. B* **54**, 11 145 (1996).